

Counter-regulation of T cell effector function by differentially activated p38

Muhammad S. Alam,¹ Matthias M. Gaida,¹ Youichi Ogawa,² Antonios G.A. Kolios,^{3,4} Felix Lasitschka,⁵ and Jonathan D. Ashwell¹

¹Laboratory of Immune Cell Biology, Center for Cancer Research; ²Dermatology Branch, Center for Cancer Research, National Cancer Institute, National Institutes of Health, Bethesda, MD 20892

³Department of Dermatology, University Hospital Zurich, 8091 Zurich, Switzerland

⁴Laboratory of Applied Immunobiology, University of Zurich, 8006 Zurich, Switzerland

⁵Institute of Pathology, University Hospital Heidelberg, 69120 Heidelberg, Germany

Unlike the MAP kinase (MAPK) cascade that phosphorylates p38 on the activation loop, T cell receptor (TCR) signaling results in phosphorylation on Tyr-323 (pY323, alternative pathway). Using mice expressing p38 α and p38 β with Y323F substitutions, we show that alternatively but not MAPK cascade-activated p38 up-regulates the transcription factors NFATc1 and IRF4, which are required for proliferation and cytokine production. Conversely, activation of p38 with UV or osmotic shock mitigated TCR-mediated activation by phosphorylation and cytoplasmic retention of NFATc1. Notably, UVB treatment of human psoriatic lesions reduced skin-infiltrating p38 pY323⁺ T cell IRF4 and IL-17 production. Thus, distinct mechanisms of p38 activation converge on NFATc1 with opposing effects on T cell immunity, which may underlie the beneficial effect of phototherapy on psoriasis.

CORRESPONDENCE

Jonathan D. Ashwell:
jda@pop.nci.nih.gov

Abbreviations used: DKI, double knock-in; GSK, glycogen synthase kinase; JNK, Jun N-terminal kinase; MAPK, MAP kinase; MAPKK, MAPK kinase.

The mitogen-activated protein kinase (MAPK) p38 has a critical role in proinflammatory responses (Lu et al., 2010; Jirmanova et al., 2011; Noubade et al., 2011). Like all MAPKs, p38 is activated by a cascade in which upstream MAPK kinases (MAPKKs) phosphorylate Thr-180 and Tyr-182 in the activation loop (dual phosphorylation, the classical pathway) leading to p38-mediated phosphorylation of substrates involved in enhanced gene transcription and mRNA stability (Pearson et al., 2001; Wu et al., 2003). T cells possess an additional activation pathway downstream of the TCR in which the tyrosine kinase Zap70 phosphorylates p38 on Tyr-323, leading to automonophosphorylation of Thr-180 (monophosphorylation of the activation loop, the alternative pathway; Salvador et al., 2005; Mittelstadt et al., 2009). Studies with dual versus monophosphorylated p38 have shown that the potency and substrate fine-specificity of these forms differ (Mittelstadt et al., 2009), raising the possibility that these two phosphorylated species may have different roles in vivo.

Alternatively activated p38 plays an important role in T cell-mediated autoimmunity. For example, Gadd45 α is a constitutive inhibitor of Tyr-323-phosphorylated (pY323) p38, and in its absence chronic activation of alternatively

activated T cell p38 results in autoimmune vasculitis (Salvador et al., 2002). Conversely, inactivation of the alternative pathway by replacing endogenous p38 α and p38 β with mutants with a Tyr \rightarrow Phe substitution at residue 323 (double knock-in [DKI] mice) prevents autoimmunity in Gadd45 α knockout mice and reduces disease severity in the murine disease models experimental autoimmune encephalomyelitis (EAE) and collagen-induced arthritis (CIA; Jirmanova et al., 2011). In this regard, Th17 cells constitute a CD4⁺ T helper subtype that mediates both protective and harmful immune responses (Korn et al., 2009). Whereas Th17 cells provide protection in response to infections such as *Klebsiella pneumoniae* (Aujla et al., 2008) and *Citrobacter rodentium* (Curtis and Way, 2009), robust Th17 activity is a major contributor to autoimmune diseases such as multiple sclerosis (Kebir et al., 2007) and rheumatoid arthritis (Pernis, 2009), as well as the autoimmune models EAE and CIA (Nakae et al., 2003; Komiyama et al., 2006). Th17 differentiation is achieved by stimulation via the TCR in combination with

This article is distributed under the terms of an Attribution-Noncommercial-Share Alike-No Mirror Sites license for the first six months after the publication date (see <http://www.rupress.org/terms>). After six months it is available under a Creative Commons License (Attribution-Noncommercial-Share Alike 3.0 Unported license, as described at <http://creativecommons.org/licenses/by-nc-sa/3.0/>).

IL-6 and TGF β , with subsequent survival promoted by IL-23 (Bettelli et al., 2006; Zhou et al., 2007), and the effects of activated Th17 cells are mediated via effector cytokines such as IL-17 and IL-22 (Korn et al., 2009). In addition to retinoic acid-related orphan receptor ROR γ t (encoded by *Rorc*), ROR α , c-Maf, and AhR (aryl hydrocarbon receptor), recent discoveries have implicated IRF4 as playing a key role in Th17 differentiation (Brüstle et al., 2007; Veldhoen et al., 2008; Yang et al., 2008; Korn et al., 2009; Sato et al., 2011). Importantly, IRF4 has been shown to bind the IL-17A promoter and induce its activity (Mudter et al., 2011). Although alternatively activated p38 has been implicated as a positive regulator of Th17 differentiation (Jirmanova et al., 2011; Noubade et al., 2011), the molecular mechanism, and in particular the role of p38 in induction of these transcription factors, is unknown.

Nuclear factor of activated T cells (NFAT) family member activity is required for many T cell effector functions, and cyclosporin A (CsA), a pharmacological inhibitor of the NFAT signaling pathway, inhibits IRF4 expression (Cristillo and Bierer, 2002) and Th17 differentiation (Cho et al., 2007; Zhang et al., 2008). The NFAT family consists of five members: NFATc1 (also known as NFATc or NFAT2), NFATc2 (also known as NFATp or NFAT1), NFATc3 (also known as NFAT4 or NFATx), NFATc4 (also known as NFAT3), and NFAT5. Except for NFAT5, which is activated by osmotic stress, NFAT family members are activated by calcium signaling (Macian, 2005). In the resting state, NFAT proteins are phosphorylated on multiple serine residues by kinases such as glycogen synthase kinase 3 (GSK3), casein kinase 1 (CK1), and the stress kinases p38 and Jun N-terminal kinases (JNK; Chow et al., 2000; Porter et al., 2000; Macian, 2005). NFAT phosphorylation results in cytosolic retention due to masking of nuclear localization sequences, exposure of a nuclear export sequence, and/or binding to cytoplasmic proteins such as 14-3-3 (Chow and Davis, 2000). Stimuli that lead to increased intracellular Ca²⁺ levels activate the phosphatase calcineurin, which dephosphorylates NFATs and allows them to migrate to the nucleus and regulate the transcription of target genes (Macian, 2005). Although the main mode of NFAT regulation is via calcium and calcineurin, NFATc1 is uniquely regulated in T cells at the transcriptional level, being up-regulated by mitogenic stimuli (Macian, 2005).

Although the alternative T cell p38 activation pathway has been implicated in T cell responses *in vitro* and *in vivo*, the molecular mechanisms by which it mediates its actions are unknown. Moreover, why TCR signaling utilizes a unique pathway, and not the conventional MAP kinase cascade (as it does for the MAPK ERK, for example; Koike et al., 2003) is an unanswered question. Here, we explored these issues and found that alternatively activated p38 is required for induction of the key transcription factors NFATc1 and IRF4 and downstream differentiation and effector functions of Th17 cells. Moreover, these responses were antagonized by MAPK cascade-activated p38 because of phosphorylation, cytoplasmic sequestration, and inactivation of NFATc1. This was also

manifested in human psoriatic lesions, in which IL-17A production by p38 pY323⁺-infiltrating T cells was greatly reduced by treatment with UV.

RESULTS

p38 alternative activation is required for TCR-induced up-regulation of NFATc1 and IRF4

The p38 alternative activation is an important step for TCR-signaled T cell proliferation, differentiation, and effector function (Jirmanova et al., 2009, 2011). To determine which genes are downstream of this form of activated p38, a cDNA microarray analysis was performed on CD4⁺ T cells from WT and DKI mice stimulated with anti-CD3/CD28. From among the ~100 genes that were decreased 1.5-fold or more in DKI compared with WT cells, 12 of the of annotated genes were of immunological interest, and one-third of these have been identified as downstream of the NFAT family of transcription factors. For example, expression of Apobec3, a cytidine deaminase whose human analogue, APOBEC3G, is regulated by NFATc1 and IRF4 and is a key molecule in antiviral immunity (Farrow et al., 2011), was roughly fourfold higher in WT compared with DKI T cells. Other NFAT-regulated targets such as Thioredoxin 1 (encoded by *Txn1*), which inhibits cellular TNF liberation by suppressing the protease ADAM17 (Aragão et al., 2012), and Schlafen 1 (encoded by *Slfn1*), which is involved in T cell development (Schwarz et al., 1998; Blomberg et al., 2009), were also expressed at lower levels in DKI than WT T cells, as was *Irf4*. The diminished expression of Apobec3 mRNA and protein in DKI T cells was confirmed by real-time PCR and immunoblotting (unpublished data), validating the microarray results that it is indeed downstream of and utilizes the p38 alternative pathway.

The finding that up-regulation of several NFAT-dependent genes was decreased in TCR-signaled DKI T cells prompted us to first ask if expression of NFATc1, the only family member that is induced at the transcriptional level, and IRF4, also upstream of cytokine expression, are regulated by p38 in T cells. Anti-CD3 induced NFATc1 and IRF4 up-regulation in CD4⁺ T cells was prevented by SB203580, a p38 α and p38 β catalytic inhibitor (Fig. 1 A). The effect was specific in that up-regulation of another inducible IRF family member, IRF8, was not prevented by inhibiting p38. To determine if p38-dependent up-regulation of IRF4 is independent, or downstream, of NFAT, CD4⁺ T cells were stimulated via the TCR in the presence of the cell-permeable, NFAT-specific inhibitor 11R-VIVIT. Induction of IRF4 mRNA (Fig. 1 B) and protein (Fig. 1 C) was prevented by 11R-VIVIT but not the inactive peptide 11R-VEET. The contribution of alternatively activated as opposed to MAPK cascade-activated p38 was addressed with CD4⁺ T cells from DKI mice. Induction of NFATc1 and IRF4 was markedly impaired in DKI CD4⁺ T cells at both the mRNA (Fig. 1 D) and protein (Fig. 1 E) levels. In contrast, expression of other NFAT (*Nfat2*, *Nfat3*, and *Nfat5*) and IRF (*Irf8*) family members did not differ between TCR-stimulated WT and DKI mice (unpublished data). Remarkably, stimulation with PMA and ionomycin,

which bypasses the TCR and activates p38 via the MAPK cascade, induced much less NFATc1 and IRF4 compared with stimulation via the TCR (Fig. 1 E). Blockade of NFAT pathway by CsA impairs IFN- γ and IL-17 expression and Th17 development (Granelli-Piperno et al., 1984; Tsuda et al., 2012). Moreover, CsA inhibits the expression of the transcription factor IRF4, and Th17 development is blocked

in IRF4 knockout mice (Cristillo and Bierer, 2002; Brüstle et al., 2007; Tsuda et al., 2012). Therefore, the ability of stimulation via the TCR versus PMA plus ionomycin to skew CD4⁺ T cells was investigated. As shown in Fig. 1 F, naive CD4⁺ T cells cultured under neutral (Th0) or Th17-skewing (Th17) conditions expressed more IFN- γ and IL-17A (both in terms of numbers of positive cells and the amount of cytokine produced),

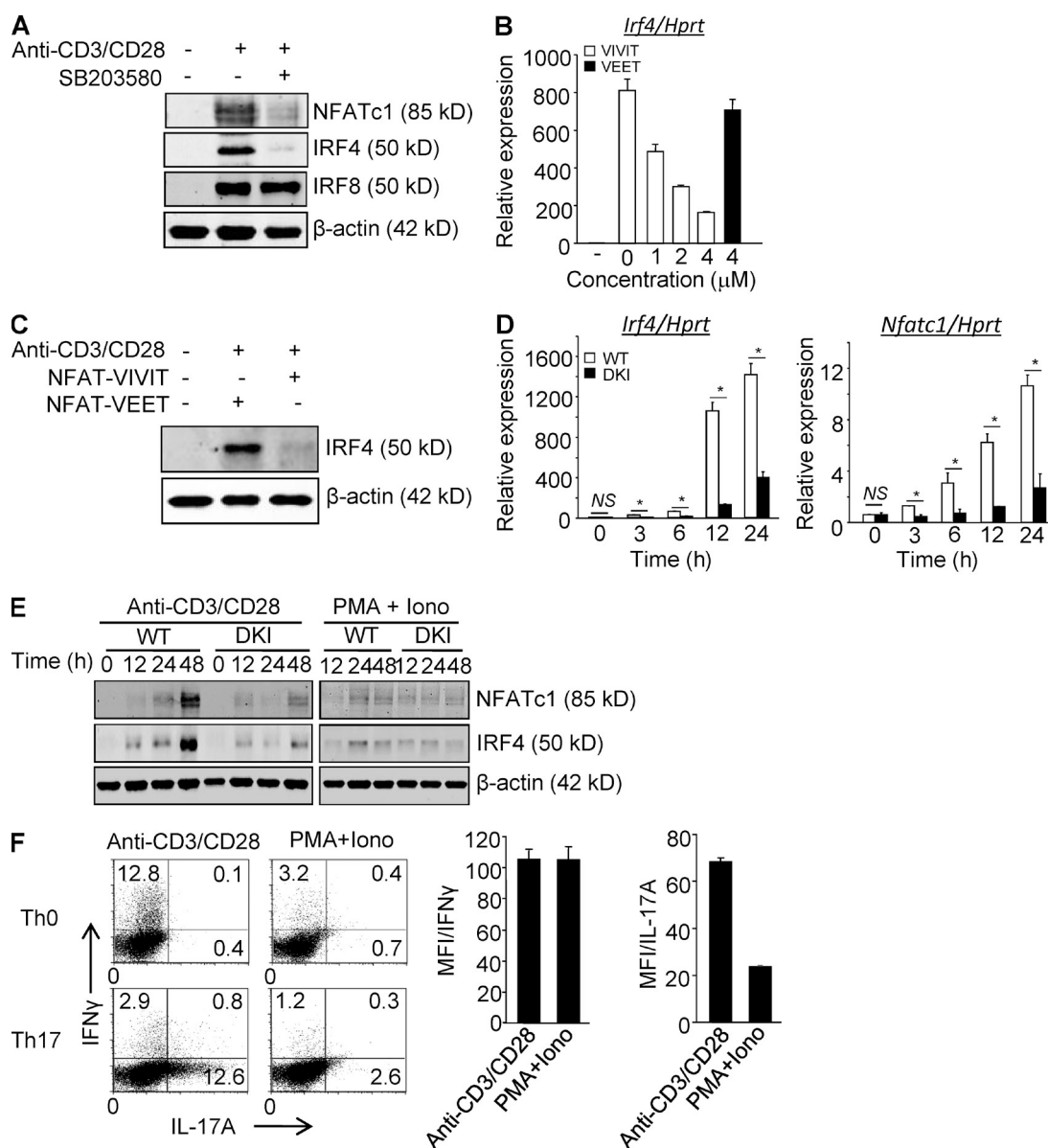


Figure 1. p38 Alternative activation is required for TCR-induced expression of NFATc1 and IRF4 in CD4⁺ T cells. (A) Purified CD4⁺ T cells were stimulated with anti-CD3/CD28 in the presence or absence of SB203580 and immunoblotted for the indicated transcription factors 48 h later. (B and C) Purified CD4⁺ T cells were stimulated with anti-CD3/CD28 in the presence of 11R-VIVIT or 11R-VEET. *lrf4* mRNA (B) and protein (C) were determined 24 h later. (D and E) Purified CD4⁺ T cells from WT and DKI mice were stimulated with anti-CD3/CD28 or PMA plus ionomycin, as indicated for the indicated times and analyzed for expression of *Nfatc1* and *lrf4* mRNA (D) and protein (E). Results shown in A–E are representative of three independent experiments each. (F) Naive CD4⁺ T cells were stimulated with either anti-CD3/CD28 or PMA and ionomycin under neutral or Th17-skewing conditions for 3 d. IL-17A and IFN- γ expression were determined by intracellular staining and flow cytometry after restimulation with PMA and ionomycin. Results shown in the left panel are representative of three independent experiments and bar graphs in the right panel show the mean \pm SEM of all three. *, $P < 0.05$ (unpaired two-tailed Student's *t* test).

respectively, when skewing was performed in the presence of anti-CD3/CD28 compared with PMA and ionomycin at a concentration that results in robust T cell activation (see also Fig. 4 C, right). Together, these results indicate that activation of p38 via the TCR, but not the MAPK cascade, is required for induction of NFATc1 and IRF4 and efficient cytokine production.

DKI mice have a defective Th17 response to *Citrobacter rodentium*

To test the importance of p38 alternative activation in a physiological setting, WT and DKI mice were infected with

C. rodentium, for which Th17 cells plays a critical protective role (Curtis and Way, 2009). Mice were analyzed at 11–12 d after infection, which is normally at or near the peak of the response (Johnson and Barthold, 1979). WT mice had more infiltrating lymphocytes in the colonic lamina propria (LP) than DKI mice (Fig. 2 A), and freshly isolated LP CD4⁺ T cells from DKI mice expressed much lower levels of *Rorc* and *Irf4*, transcription factors required for Th17 differentiation, than their WT counterparts (Fig. 2 B). Correspondingly, *Il17a* mRNA and protein expression was highly impaired in lamina propria CD4⁺ DKI T cells (Fig. 2, B and C). In agreement with

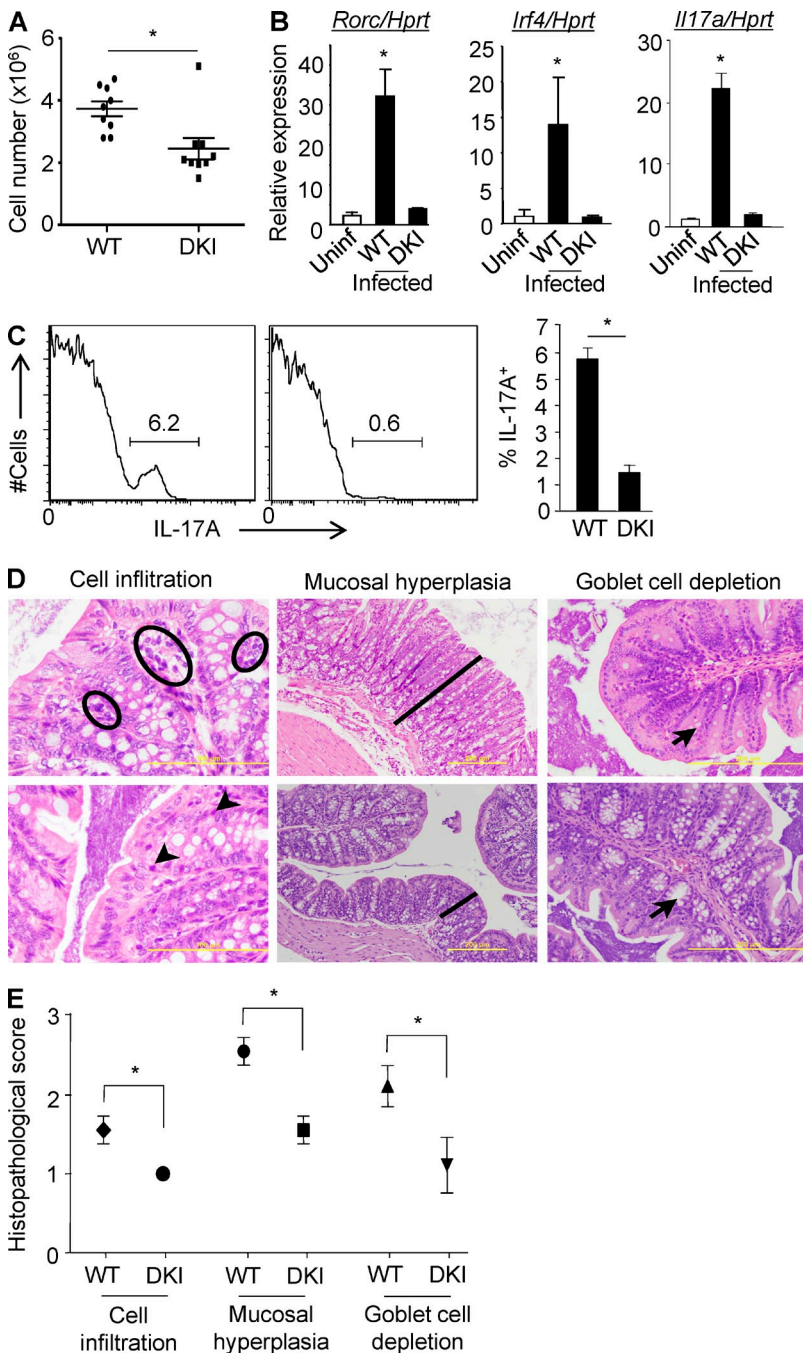


Figure 2. DKI mice have a defective Th17 response to infection with *C. rodentium*. (A) WT and DKI mice were infected with *C. rodentium* by gavage and at day 11–12 cells in the LP were counted. Each symbol represents one mouse, and the mean ± SEM are shown. Data are pooled from two independent experiments with a total of nine mice per group. (B) At day 11 after infection, CD4⁺ T cells were purified and the expression of *Il17a*, *Rorc*, and *Irf4* were determined by real-time PCR. The means ± SD are shown (*n* = 5 mice per group from two independent experiments). (C) IL-17A expression by LP CD4⁺ T cells was determined by intracellular staining 4 h after stimulation with PMA and ionomycin (left). The mean percentage ± SD of IL-17A-producing CD4⁺ T cells is shown (right, *n* = 5 mice per group). Data are representative of two independent experiments. (D) Histological evaluation of representative H&E-stained slides of the colon from WT and DKI mice on day 11 of infection (*n* = 9 mice per group from 2 independent experiments). Accumulations of lymphocytes are indicated with black circles in WT or arrowheads in DKI mice (left, bar: 100 μm). The thickness of the mucosa is indicated with a black line (middle, bar: 200 μm). Black arrows indicate goblet cells in the colon mucosa (right, bar: 200 μm). (E) The histopathological parameters were quantitated using a double-blinded visual scoring system as detailed in Materials and methods. Data are pooled from 2 independent experiments with a total of 9 mice per group. *, *P* < 0.05 (unpaired two-tailed Student's *t* test).

the *in vitro* analyses, histological examination revealed much greater signs inflammation in the colons of WT compared with DKI mice, with greater lymphocyte infiltration in the LP (Fig. 2 D, left), increased mucosal thickness and hyperplastic and elongated crypts, sometimes with a pseudostratified appearance and obvious increased mitotic activity of enterocytes (Fig. 2 D, middle), as well as marked goblet cell depletion (Fig. 2 D, right). A semiquantitative histopathological analysis of multiple mice confirmed the diminished inflammation in the gut of DKI mice (Fig. 2 E).

MAPK-cascade activation of p38 inhibits functions mediated by alternatively activated p38

The existence of a TCR signaling-specific p38 activation pathway raises the possibility that activation of p38 via the otherwise universal mechanism, the MAPK cascade, is ineffective or even detrimental to functional responses, either of which is consistent with the finding that PMA plus ionomycin is a poor inducer of p38-dependent NFATc1 and IRF4 (Fig. 1 E). To ask if classical activation is detrimental, CD4⁺ T cells were treated with stimuli that initiate the MAPK cascade by different mechanisms to activate p38: sorbitol (osmotic stress), low dose UVB (radiation), and PMA and ionomycin (Fig. 3 A). Whereas none of these stimuli up-regulated NFATc1 or IRF4 mRNA, they inhibited TCR-mediated alternative pathway up-regulation of NFATc1 and IRF4 mRNA (Fig. 3 B) and IRF4 protein (Fig. 3 C). This was not because of toxicity, because these treatments caused little to no reduction in cell viability compared with medium alone (unpublished data). NFAT family members are inactivated by phosphorylation, which results in their retention in the cytosol, and NFATc1 is a known substrate for p38 *in vitro* and *in vivo* (Porter et al., 2000). Indeed, in TCR-stimulated primary T cells NFATc1 was found predominantly in the nucleus, where it is active, and the cytosolic fraction migrated more slowly (~5 kD) when resolved on 8% SDS-PAGE, reflecting its higher degree of phosphorylation (Fig. 3 D). The effect of MAPK cascade-activated p38 on NFATc1 activation was determined by stimulating CD4⁺ T cells with anti-CD3/CD28 for 48 h to allow up-regulation of NFATc1 expression, and then treatment with medium or sorbitol for 30 min followed by resting the cells for another 1 h. TCR-mediated activation induced accumulation of NFATc1 in the cytosol and the transcriptionally active nuclear fraction (Fig. 3 E). Strikingly, osmotic stress caused egress of NFATc1 from the nucleus to the cytosol, which was largely prevented by addition of the p38 inhibitor SB203580 just before sorbitol treatment. Notably, inhibition of the other major stress kinase, JNK, by SP600125 also prevented the translocation of NFATc1 from the nucleus to the cytosol, and inhibiting both p38 and JNK was additive, resulting the greatest nuclear-to-cytosolic NFATc1 ratio. The effect of MAPK cascade activation on NFATc1 localization was even apparent when the brief sorbitol treatment was performed at the beginning of the 48-h period of activation (Fig. 3 F). In this case, sorbitol caused a reduction in total NFATc1 (compare NFATc1 in the cytosol

plus nucleus between sorbitol-treated and -untreated cells), consistent with the reduction seen in NFATc1 mRNA (Fig. 3 B). Notably, almost all of the NFATc1 that was expressed was excluded from the nuclear fraction. Therefore, activation of p38 via the MAPK cascade has acute and long-term effects on the ability TCR-mediated stimulation to induce and activate NFATc1. This raised the possibility that NFATc1, a known p38 substrate (Porter et al., 2000), may be phosphorylated by classically but not alternatively activated p38. Although not mapped in mouse cells, in human cells the phosphorylation of NFATc1 S172 is known to cause cytosolic retention (Chow et al., 2000; Porter et al., 2000). Therefore, we stimulated the human T leukemia cell line Jurkat via the TCR for 48 h, activated the MAPK cascade by treating with sorbitol for 30 min, and, after a 1-h rest, immunoblotted the cytosolic fraction with antibodies specific for phospho-S172 NFATc1 (p-NFATc1; Fig. 3 G). Whereas stimulation via the TCR caused only a small increase in p-NFATc1, sorbitol treatment resulted in high levels. Similar to mouse CD4⁺ T cells, inhibition of either p38 or JNK reduced the phosphorylation to background levels, and inhibition of both resulted in even lower levels. Consistent with its role in preventing nuclear translocation, p-NFATc1 was undetectable in the nuclear fractions of these cells (unpublished data). Importantly, whereas Zap70-activated p38 (p38 pY323) phosphorylated ATF2 (a substrate common to both classically and alternatively activated p38), as well as MKK6-activated p38 (Fig. 3 H), there was a striking difference in their ability to phosphorylate NFATc1 (Fig. 3 I). NFATc1 S172 is known to be phosphorylated by JNK (Chow et al., 2000). To determine if classically activated p38 can directly target this residue, an *in vitro* kinase assay using recombinant material was performed. As shown in Fig. 3 J, NFATc1 S172 was phosphorylated by both kinases, consistent with the inhibitor data showing a contribution of both in the retention of NFATc1 in the cytosol. The appearance of phosphorylated S172 was accompanied by a shift in the migration of the recombinant NFATc1, another indication of its phosphorylation (Fig. 3 K). Therefore, NFATc1 phosphorylation and inactivation is performed by classically activated but not alternatively activated p38.

Stress-mediated activation of p38 interferes with TCR-mediated responses

To determine the functional consequences of MAPK cascade activation, CD4⁺ T cells were exposed to sorbitol, and then cultured under Th17-skewing conditions using anti-CD3/CD28. Sorbitol treatment resulted in substantially reduced *Ifi4* and *Rorc* mRNA (Fig. 4 A), IL-17A protein (Fig. 4 B), *Tbet* (Fig. 4 C), and IFN- γ (Fig. 4 D). The reduced cytokine secretion was not due to diminished CD4⁺ T cell activation, *per se*, because sorbitol treatment had no effect on TCR-induced up-regulation of the activation markers CD69 and CD25 (unpublished data). Furthermore, sorbitol treatment markedly reduced proliferation of CD4⁺ T cells to anti-CD3/CD28, likely because IRF4 is a positive regulator of T cell proliferation and effector function (Lohoff et al., 2002; Tominaga et al.,

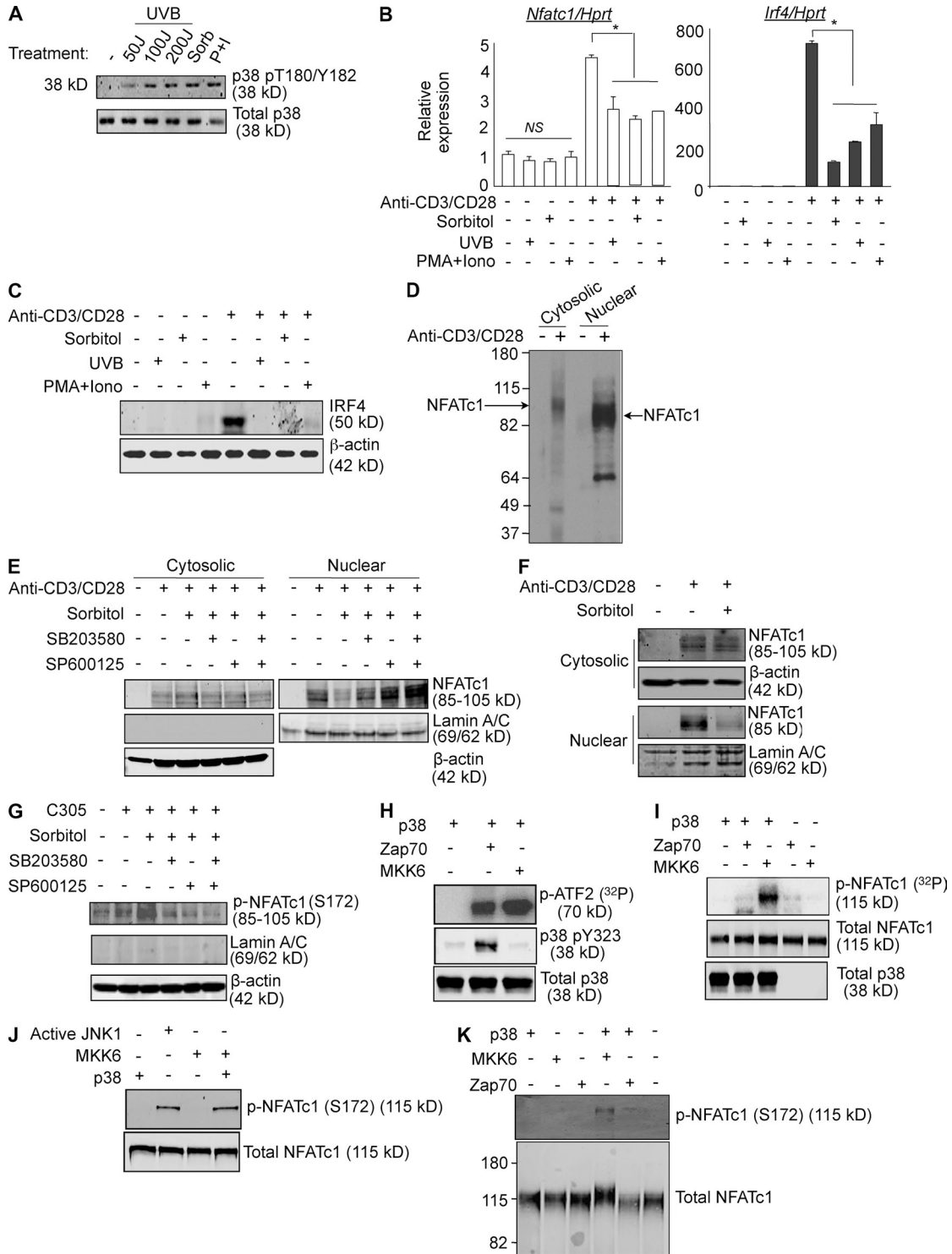


Figure 3. MAPK-cascade activated p38 inhibits functions distal to alternatively activated p38. (A) Purified CD4⁺ T cells were cultured overnight without stimulation, and then treated with either UV (50 J/m² or 100 J/m² or 200 J/m²), 0.6 M sorbitol for 30 min, or PMA (10 ng/ml) and ionomycin (1 μg/ml) for 1 h. Cell lysates were immunoblotted with anti-phospho-p38. The results are representative of three independent experiments. (B) Purified CD4⁺ T cells were treated with either 0.6 M sorbitol for 30 min, 50 J/m² UV, or PMA and ionomycin were stimulated with anti-CD3/CD28 for 24 h. The expression of *Nfatc1* and *Irf4* was determined by quantitative real-time PCR. Results are the mean ± SEM of three independent experiments. *, P < 0.05 (unpaired two-tailed Student's *t* test). (C) Cells were treated as in B, and IRF4 expression was determined by Western blot. The results are representative of two independent experiments. (D) Freshly purified T cells were stimulated or not with anti-CD3/CD28 for 48 h. Cytosolic and nuclear fractions were separated in a low percentage SDS-PAGE (8%) gel and immunoblotted for NFATc1. The results are representative of three independent experiments. (E) CD4⁺

2003; Brüstle et al., 2007; Fig. 4 E, left). This was not due to a toxic effect of osmotic stress, because the same T cells proliferated normally when stimulated with PMA and ionomycin, which bypasses the TCR, and thus the alternative p38 pathway (Fig. 4 E, right).

Effect of UV on skin-infiltrating T cell activation

To ask if activation of p38 via a stress pathway could affect T cell responses in a biologically relevant setting, we characterized p38 activation and *Irf4*-induction in T cells from UV-treated skin. Once after exposure to the minimum erythema dose (MED) of UV there was a marked increase in dual-phospho p38 in keratinocytes, dermal fibroblasts, and skin-resident T cells (Fig. 5 A). Strikingly, TCR-mediated stimulation of CD4⁺ T cells isolated from UV-treated skin induced *Irf4* at much lower levels than in T cells from untreated skin, whereas there was relatively little effect on *Irf8* (Fig. 5 B).

Psoriasis is a Th17-dependent inflammatory disease of the skin that is responsive to treatment with UV (phototherapy; Grundmann-Kollmann et al., 2002; Rácz et al., 2011). Given the finding that UV inhibited TCR-induced *Irf4*-induction in skin-resident T cells, we asked if the p38 alternative pathway is active in skin-infiltrating T cells in human psoriatic lesions. Skin sections of patients with active psoriasis were stained with antibodies specific for p38 pY323. Whereas no staining was detected in T cell-poor areas, in T cell-rich regions the majority of cells expressed Y323-phosphorylated p38 (Fig. 5 C). Given that pY323 is generated only in response to TCR-mediated signals, this argues strongly that the skin-infiltrating cells are actively responding to local antigens. To determine if UV therapy interfered with the consequences of alternative p38-dependent T cell signaling, we examined biopsies taken from patients pre- or post-treatment with UVB. Fluorescent staining found that >20% of the p38-pY323 cells also expressed IRF4 and IL-17A (triple positive), indicating that the major source of IL-17A in the affected skin was from TCR-activated T cells (Fig. 5 D, top). After a cycle of treatment with UVB, the number of p38-pY323⁺ cells was unchanged, demonstrating that UV had little or no effect on T cell infiltration or TCR-mediated p38 activation. Strikingly,

however, far fewer of the activated T cells expressed IRF4 or IL-17A (Fig. 5 D, middle). Quantitation of biopsies from five pretreatment and three post-treatment psoriasis patients revealed that although UVB did not reduce the number of pY323⁺ infiltrating T cells, it caused a statistically significant reduction in the fraction that produced IRF4 and IL-17A (Fig. 5 E), consistent with the ability of dual-phospho p38 to inhibit effector functions dependent on mono-phospho p38.

DISCUSSION

There is a great deal of evidence supporting a critical role for p38 in autoimmunity and inflammation (Lu et al., 2010; Jirmanova et al., 2011; Noubade et al., 2011), but little is known about the mechanism by which T cell p38, and in particular the alternative activation pathway downstream of TCR occupancy, contributes. Using pharmacologic and genetic approaches, we have found that the Zap70-mediated p38 alternative activation pathway is required for up-regulation of NFATc1 and IRF4, critical transcription factors for proinflammatory cytokine production, in TCR-activated primary T cells in vitro and in vivo. This is in agreement with previous indirect evidence showing that Dlg1, a p38-binding scaffold protein involved in activation of the alternative pathway, plays a positive role in TCR-mediated induction of NFATc1 (Round et al., 2007). Notably, activation of the p38 via the MAPK cascade was incapable of causing NFATc1 and IRF4 up-regulation, and actually antagonized the action of alternatively activated p38. These observations provide a satisfying explanation for why T cells have acquired a unique p38 activation pathway: to allow induction of biologically important transcriptional events that would otherwise be prevented by MAPK cascade-activated p38. They also resolve the paradox that phosphorylation of NFATc1 by p38 has been shown to cause its inactivation by retention in the cytosol, yet p38 is essential for the production of many NFATc1-dependent cytokines in TCR-activated T cells (Wu et al., 2003). The answer lies in the finding that unlike MKK-phosphorylated p38, NFATc1 is a poor substrate for Zap70-phosphorylated p38. Therefore, TCR signaling does not inhibit NFATc1-dependent transcriptional activity. We found that inhibition of JNK,

T cells were stimulated for 48 h with anti-CD3/CD28, and then treated with sorbitol in the presence or absence of SB203580 and/or SP600125 for 30 min, rested for 1 h, then immunoblotted for NFATc1 in cytosolic and nuclear fractions. Results are representative of three independent experiments. (F) Purified CD4⁺ T cells were treated or not with sorbitol for 30 min and stimulated with anti-CD3/CD28 for 48 h, and then immunoblotted for NFATc1 in cytosolic and nuclear fractions. The results are representative of three independent experiments. (G) Jurkat T cells were stimulated for 48 h with an agonistic anti-TCR antibody (C305), and then treated with sorbitol in the presence or absence of SB203580 and/or SP600125 for 30 min. After 1 h without further stimulation, cytosolic fractions were immunoblotted for phospho-NFATc1 (p-NFATc1). The results are representative of three independent experiments. (H) Recombinant p38 was activated with Zap70, MKK6, or buffer alone in in vitro kinase buffer. After 1 h, recombinant ATF2 and 10 μ Ci [³²P]ATP were added for 30 min before separation on SDS-PAGE and PhosphorImager analysis. The phosphorylation state of p38 Y323 was determined by immunoblotting. The results are representative of three independent experiments. (I) Recombinant p38 was activated with Zap70, MKK6, or buffer alone and an in vitro kinase assay using recombinant NFATc1 as substrate was performed as in (H). The results are representative of two independent experiments. (J) Recombinant p38 was activated with MKK6 or buffer alone in in vitro kinase buffer. Active JNK1 was kept in in vitro kinase buffer. After 1 h, recombinant NFATc1 was added and incubated for an additional hour before separation on SDS-PAGE and immunoblotting with an antibody specific for NFATc1 phosphorylated on residue S172. The results are representative of two independent experiments. (K) Recombinant p38 was activated with Zap70, MKK6, or buffer alone in an in vitro kinase assay with recombinant NFATc1 as the p38 substrate, as in I. Samples were separated on a low percentage SDS-PAGE (8%) and immunoblotted for NFATc1 phosphorylated on residue S172. The results are representative of three independent experiments.

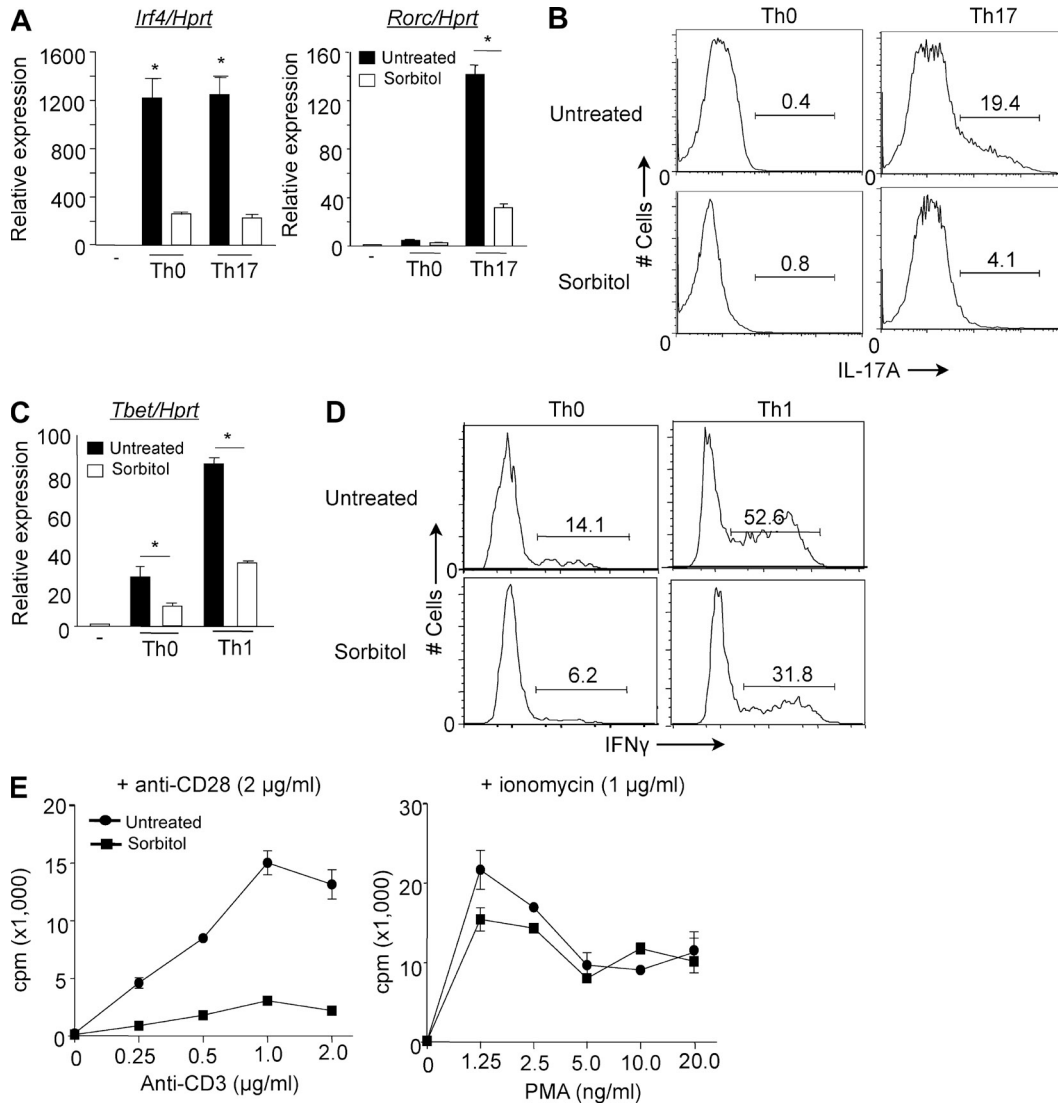


Figure 4. MAPK cascade-activated p38 inhibits T cell proliferation and effector function mediated by alternatively activated p38. (A and B) Naive CD4⁺ T cells were treated with 0.6 M sorbitol for 30 min or untreated, and then stimulated with anti-CD3/CD28 in neutral or Th17-skewing conditions. After 2 d, *Irf4* and *Rorc* mRNA levels were analyzed by quantitative real-time PCR (A), and after 3 d, IL-17A expression was determined in cells restimulated with PMA and ionomycin for 4 h. (B) The numbers indicate the frequency of IL-17A-producing cells. The results are representative of two independent experiments. (C and D) Naive CD4⁺ T cells were treated as in A, and then stimulated with anti-CD3/CD28 either in neutral (Th0) or Th1 skewing conditions for 2 d, at which time *Tbet* mRNA was measured by real-time PCR (C), and after 3 d cells were restimulated with PMA and ionomycin for 4 h and intracellular IFN- γ expression was measured by flow cytometry (D). The numbers indicate the frequency of IFN- γ -producing cells. *, $P < 0.05$ (unpaired two-tailed Student's *t* test). Data are representative of at least three independent experiments. (E) T cells were stimulated with the indicated concentrations of anti-CD3 in the presence of anti-CD28 (wells coated with 2 $\mu\text{g/ml}$) or PMA and ionomycin for 48 h and proliferation was assessed by [³H]thymidine incorporation. Data shown are representative of at least three independent experiments.

another stress kinase that can phosphorylate NFATc1 S172 (Chow et al., 2000), also had a partial effect on NFATc1 nuclear translocation. Although we can't exclude the possibility that stress-activated signaling events other than p38 and JNK activation might influence NFATc1 translocation, our finding that inhibition of both p38 and JNK almost completely prevented NFATc1 retention in the cytosol suggests that these two kinases are the major contributors to stress-induced NFATc1 inhibition. The molecular events downstream of alternatively

but not MAPK cascade-activated p38 that result in up-regulation of *Nfatc1* transcription remain to be determined.

The results in this study show that TCR-induced NFATc1/IRF4-dependent IL-17 production is mediated by the alternative p38 activation pathway. There are other, perhaps non-physiologic, means one can use to achieve IL-17 production as well. This is indicated by the ability of PMA and ionomycin, which bypass proximal TCR signaling, to activate the classical p38 cascade and, although doing so less well, inducing

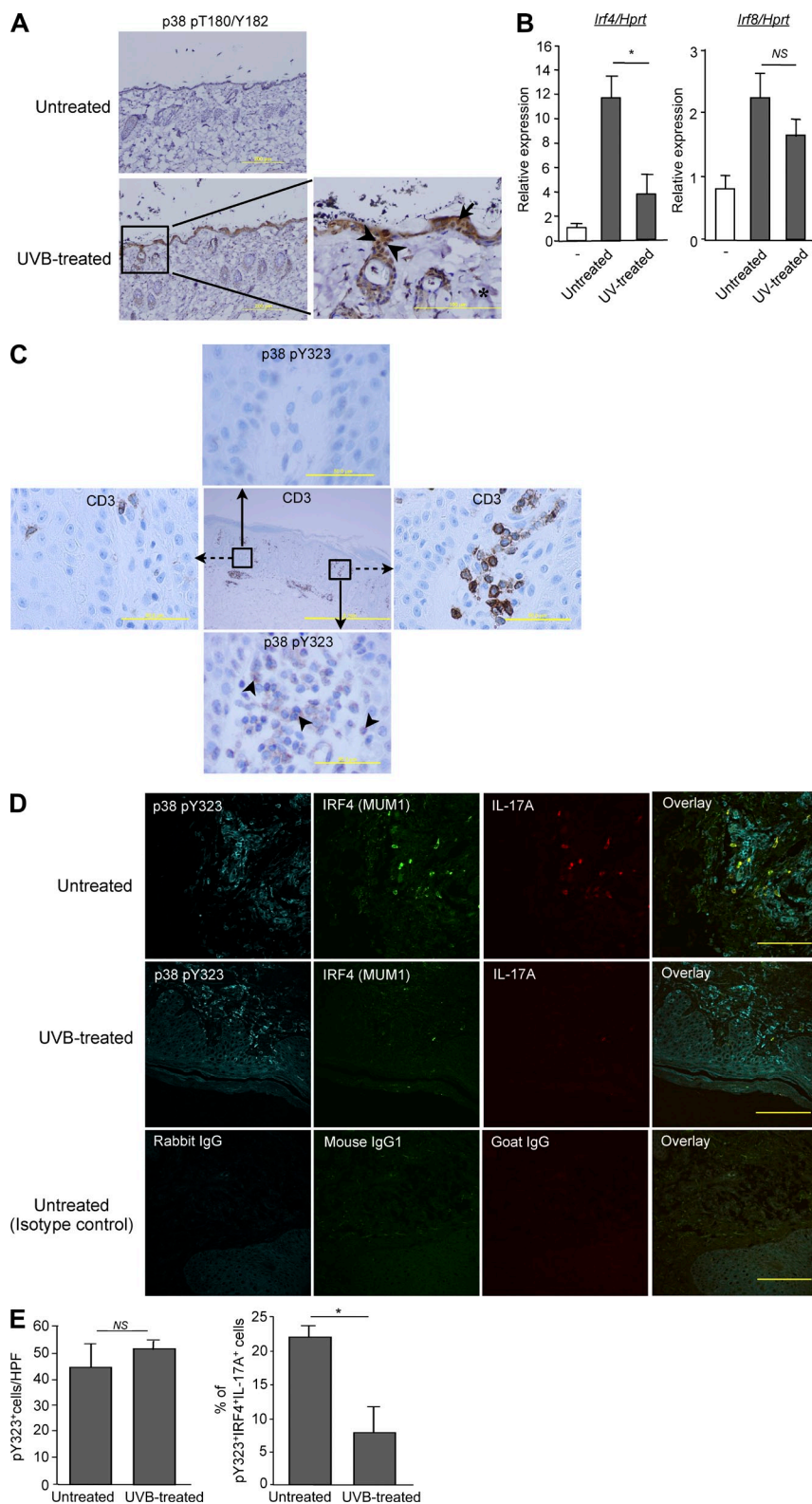


Figure 5. Effect of UV on skin-infiltrating T cells. (A) Mice were exposed or not to UV radiation as described in Materials and methods and, 1 h later, skin sections were obtained and immunostained for CD3 (not depicted) and dual phospho-p38 (pT180/pY182). Phospho-p38-positive T cells are indicated with arrowheads, keratinocytes with arrows, and dermal fibroblasts with asterisks. Bars: 200 μ m (left); 100 μ m (right). Data are representative of five mice per group from two independent experiments. (B) Purified CD4⁺ T cells from the skin of UV treated or untreated mice were stimulated in vitro with anti-CD3/CD28 for 24 h, and *Irf4* mRNA expression was measured by real-time PCR. Results are the mean \pm SEM of two independent experiments with a total of 5 mice per group. *, $P < 0.05$, NS, not statistically significant (unpaired two-tailed Student's *t* test). (C) Immunohistochemical staining of human psoriatic skin lesions with anti-CD3 or phospho-p38 Y323 (p38 pY323)-specific antibodies. The insets in the middle pane show the T cell-poor and T cell-rich areas that are enlarged in the left and right panes for CD3 and the top and bottom panes for p38 pY323. Arrows indicate examples of p38 pY323-positive cells ($n = 3$ patients; Bars: 1 mm (middle); 50 μ m (outer panels)). (D) Immunofluorescence staining for p38 pY323 (cyan), IRF4 (green), IL-17A (red), and the corresponding isotype control of representative psoriatic skin lesions biopsies before and after UVB treatment (Bar, 100 μ m). (E) Quantitation of p38 pY323⁺ cells that are also positive for IRF4 and IL-17A (triple positive) in the skin of 6 patients before treatment and 3 of these after UVB treatment. *, $P < 0.05$. NS, not significant (unpaired two-tailed Student's *t* test).

T cell IL-17 production despite much less NFATc1 and IRF4 up-regulation (Fig. 1, E and F). It is possible that this is because the very strong Ca²⁺ signal triggered by the calcium ionophore ionomycin activates other, constitutively expressed NFAT

family members, in particular NFATc2 (Ghosh et al., 2010). Another study described a positive role for MAPK cascade-activated p38 in T cell IL-17 production (Noubade et al., 2011). Although most of the experiments used chemical inhibitors

or dominant negative p38, which would affect p38 activated by both pathways, in some experiments MKK3-deficient and MKK6 haplozygous T cells were found to have decreased IL-17 in response to anti-CD3. Interestingly, and in distinction to the findings in the present report, it was found that MAPK cascade-activated p38 was not required in Th17-skewed cells for *Rorc* or *Il17* mRNA production, but rather for activation of the translation initiation factor eIF-4E-MNK pathway and promotion of IL-17 protein translation. Our data, on the other hand, demonstrate that the alternative p38 pathway is required for transcriptional up-regulation of *Nfatc1*, *Irf4*, *Rorc*, and *Il17a*. These are not mutually exclusive observations, and it is possible that the regulated balance of the two (transcription and translation) might have a biphasic effect on biological responses downstream of p38.

Although this study focused on IL-17, a diminished NFATc1 and IRF4 response in mice lacking the alternative p38 activation pathway would be expected to have an impact on several proinflammatory cytokines. Blastocyst complementation assays with NFATc1 knockout embryonic stem cells found that IL-4 but not TNF and IFN- γ production was diminished (Yoshida et al., 1998). Fetal liver chimeras in which both NFATc1 and NFATc2 were knocked out had more extensive cytokine deficiencies, with reductions in IL-2, IL-4, IFN- γ , and IL-5 (Peng et al., 2001). In this regard, we previously found that IFN- γ but not IL-4 expression was diminished in T cells from DKI mice, which is consistent with their rapid loss of T-bet expression after activation (Jirmanova et al., 2009). It is possible that p38 alternative activation pathway controls NFATc1 expression indirectly by promoting nuclear translocation of NFATc2 via phosphorylation of conserved residues critical for transactivation. Consistent with this, DKI T cells had impaired production of TNF (unpublished data), which is downstream of NFATc2 (Kaminuma et al., 2008), and MAPK-activated p38 is known to phosphorylate and inactivate NFATc2 (Gómez del Arco et al., 2000). Whether NFATc2 is also a substrate for alternatively activated p38, and if so at what sites, remains to be determined.

The Gram-negative bacterium *C. rodentium* (a rodent equivalent of enteropathogenic *Escherichia coli*) causes a robust colonic Th17 response by the second week after infection (Bry and Brenner, 2004; Symonds et al., 2009). Although $\gamma\delta^+$ T cells can secrete IL-17 (Poggi et al., 2009; Silva-Santos, 2011), it is IL-17-producing $\alpha\beta^+$ CD4 $^+$ T cells that play a protective role, because mice lacking CD4 $^+$ $\alpha\beta$ T cells exhibited substantial mortality when infected with *C. rodentium*, whereas mice lacking $\gamma\delta^+$ or CD8 $^+$ $\alpha\beta$ cells survived (Bry and Brenner, 2004). The finding that DKI CD4 $^+$ $\alpha\beta$ T cells in the lamina propria had diminished levels of *Rorc* and *Irf4*, and that the mice failed to mount a normal Th17 response, indicates that protective adaptive immunity to *C. rodentium* is strictly dependent on p38 activation, in particular p38 activated via TCR engagement.

The findings that cytokine responses mediated by the alternative p38 pathway are diminished by activating the classical p38 pathway may have implications for understanding the

therapeutic effects of phototherapy in clinical settings. UV has been used to treat psoriasis, a chronic T cell-mediated skin disease in which Th17 cells play a key pathological role (Fitch et al., 2007), and that therapy with anti-IL-17 or anti-IL-17R is remarkably effective (Leonardi et al., 2012; Papp et al., 2012). Initially, attention largely focused on the direct effects of UV on keratinocytes, such as induction of apoptosis and reduction of proliferation, which have been shown to be mechanisms for psoriatic plaque clearance after UVB treatment (Erkin et al., 2007; Weatherhead et al., 2011). Notably, the percentage of IFN- γ - but not IL-2-producing T cells has been shown to be decreased in the course of UVB treatment (Walters et al., 2003), which parallels the finding that production of IFN- γ but not IL-2 was reduced in TCR-stimulated DKI T cells (Jirmanova et al., 2009). In addition, skin from UV-treated patients has been reported to have reduced transcripts of genes involved in Th17 and type I and II interferon signaling (Rácz et al., 2011). Interestingly, UVB irradiation induces RANKL expression in keratinocytes and systemic immunosuppression (Loser et al., 2006). Given that RANKL has been shown to activate stress kinases like p38 by the MAPK cascade (Matsumoto et al., 2000), it is possible that RANKL produced by keratinocytes contributes to inhibition by activating the classical p38 pathway in pathogenic T cells, thereby dampening the immune response. This would be another, indirect, means by which the MAPK cascade could antagonize biological events downstream of alternatively activated p38.

In the present study, we found that the majority of cells in psoriatic lesions that were positive for IL-17A (and IRF4) were T cells in which the p38 alternative activation pathway was active. UVB treatment did not reduce the number of p38 pY323-positive cells, but did reduce their ability to produce IL-17A. The results suggest that the beneficial effects of UV radiation are, at least in part, due to activation of the classical MAPK cascade with a resulting reduction in NFATc1 activity and proinflammatory cytokine production by pathogenic T cells.

MATERIALS AND METHODS

Mice. Mice expressing p38 $\alpha\beta^{Y323F}$, in which endogenous p38 α and p38 β contain a Tyr→Phe substitution at residue 323 (double knock-in, or DKI mice; Jirmanova et al., 2011), were crossed onto C57BL/6 (B6) for at least 12 generations. Mice were maintained in the National Cancer Institute pathogen-free animal facility, and all animal experiments were performed under a National Institutes of Health-approved animal study protocol.

Cells. Primary CD4 $^+$ T cells were purified from spleens of 6–12-wk-old B6 or DKI mice using negative-selection T cell purification columns (CL101; Cedarlane). Purified CD4 $^+$ T cells were cultured in RPMI 1640 medium supplemented with 10% fetal bovine serum (Invitrogen), 2 mM glutamine, 50 μ M β -mercaptoethanol, and 100 μ M gentamicin (complete medium).

Reagents. Mouse-specific antibodies against p38 α (5F11; Cell Signaling Technology), CD4 (RM4-5; BD Biosciences), CD8 (53-6.7; BD), IL-17 (eBio17B7; eBioscience), and IFN- γ (XMG1.2; eBioscience) were used. Anti-CD3 (145-2C11) and anti-CD28 (37.51) were purchased from BD.

Phorbol myristate acetate (PMA) and ionomycin were purchased from Sigma-Aldrich. Recombinant NFATc1 protein was purchased from SignalChem and anti-NFATc1 antibody (MA3-024) was purchased from Thermo Fisher Scientific. Anti-human phospho NFATc1 (S172; clone 679340) was purchased from R&D Systems. Anti-IRF4 antibody was purchased from Cell Signaling Technology, and IRF8, from Invitrogen. Recombinant full-length NFATc1 was purchased from SignalChem. SB203580 (p38 inhibitor) and SP600125 (JNK inhibitor) were purchased from Cell Signaling Technology. [γ - 32 P]ATP was purchased from PerkinElmer.

Microarray analysis. Purified CD4⁺ T cells from WT and DKI mice were stimulated with anti-CD3/CD28 for 12 h, lysed, mRNA isolated, and reverse transcribed to cDNA, and microarray was performed using Affymetrix chips. The microarray data were analyzed by Partek software.

Intracellular cytokine staining. CD4⁺ T cells were stimulated with plate-bound anti-CD3 (2 μ g/ml) and anti-CD28 (2 μ g/ml) in Th0 (neutral), Th1 (10 ng/ml IL-12 and 10 μ g/ml anti-IFN- γ), or Th17 (20 ng/ml IL-6, 5 ng/ml TGF β , 10 μ g/ml anti-IFN- γ , and 10 μ g/ml anti-IL-4) conditions for 3 d. Skewed cells were placed in 96-well plates and restimulated with PMA (10 ng/ml) and ionomycin (1 μ g/ml) in the presence of monensin (3 μ M) for 4 h at 37°C. Cells were then washed in FACS buffer (1% BSA plus 0.1% sodium azide) and fixed and permeabilized with Cytofix/Cytoperm solution for 25 min on ice, followed by washing in Perm/Wash solution (BD). Cells were stained for 30 min at room temperature with mAbs against IL-17A and IFN- γ , washed two times in Perm/Wash solution, and once with FACS buffer, and analyzed by flow cytometry (FACSCalibur using CellQuest Pro 5.2.1 software [BD]). Data were analyzed with FlowJo 9.2 software (Tree Star).

Histopathological analysis of gut sections. Two colon samples from each mouse ($n = 9$) were collected on day 11–12 after infection with *C. rodentium*, fixed in buffered formalin, and embedded in paraffin. Paraffin blocks were cut into 4- μ m sections and stained with hematoxylin and eosin (H&E). For the semiquantification of the inflammation, a previously described scoring system (Galeazzi et al., 1999) was used with minor modifications. In brief, mucosal hyperplasia (increased mucosal thickness with crypt hyperplasia and elongation, formation of pseudoinvasive, pseudostratified, or pseudopolypous growth, increased mitotic activity) was scored as absent (0), mild (1), moderate (2), or extensive (3). Goblet cell depletion was quantified similarly (scores of 0–3). The depth of inflammatory cell infiltration was scored as absent (0), mild (1) inflammation in mucosa and submucosa, moderate (2) inflammation to the lamina muscularis propria, or severe (3) transmural inflammation.

T cell proliferation assay. Purified CD4⁺ T cells were stimulated with plate-bound α -CD3 (2 μ g/ml) and α -CD28 (2 μ g/ml) for 48 h in 96-well flat-bottomed plates. Cells were pulsed with 1 μ Ci [3 H]thymidine 14 h before harvesting. [3 H]thymidine uptake was determined with a Wallac 1450 MicroBeta Liquid Scintillation Counter.

Protein purification. Recombinant p38 α and constitutively active MKK6 (S207E/T211E) were purified as previously described (Mittelstadt et al., 2009). In brief, p38 α and MKK6 were expressed in the bacterial strain BL21(DE3) using the vector pET15b. After cultures reached an A600 of 0.5–1.0, protein expression was induced with 0.5 mM isopropyl β -D-thiogalactopyranoside (IPTG) and incubated overnight at 4°C. Cells were resuspended in ice-cold PBS, including 0.5 M NaCl, 0.1% Triton X-100, and 1 mM phenylmethylsulfonyl fluoride, sonicated, and centrifuged at 20,000 g for 20 min at 4°C. Proteins were purified with cobalt-charged chelating-Sepharose Fast Flow beads (GE Healthcare) and eluted with 0.3 M imidazole in PBS with 0.5 M NaCl. Proteins were concentrated and washed into PBS using Microcon YM-30 spin columns (Millipore).

Real-time PCR. Total RNA was extracted with RNeasy mini-kit (QIAGEN). After reverse transcription using the Omniscript RT kit (QIAGEN), Power SYBR Green premix (Applied Biosystems) was used for quantitative PCR. All

data were normalized to HPRT (hypoxanthine-guanine phosphoribosyl transferase) and were presented as relative expression to the background value. The primers used in this study for real-time PCR are as follows: Irf4-Fwd, 5'-GCAGTCACTTTGGATGACA-3', Rev, 5'-CCAAACGTACAGGACA-TTG-3'; Irf1-Fwd, 5'-GCAAAACCAAGAGGAAGCTG-3', Rev, 5'-CAG-AGAGACTGCTGCTGACG-3'; Irf8-Fwd, 5'-GATCGAACAGATCGA-CAGCA-3', Rev, 5'-GCTGGTTCAGCTTTGTCTCC-3'; Nfatc1-Fwd, 5'-CGTACCTTCCTGCCAATGTT-3', Rev, 5'-TGGTGAGCTGTTG-GCTGTAG-3'; Nfatc2-Fwd, 5'-TCTGCTGTTCTCATGGATGC-3', Rev, 5'-TCCTCTCCTCCTGCTCACAT-3'; Nfatc3-Fwd, 5'-TCCAC-TTGAGCCATCCTACC-3', Rev, 5'-AGAGCCACCTGGAGAAG-TCA-3'; Nfat5-Fwd, 5'-GCGGACAGTATCCGGTAAAA-3', Rev, 5'-TGCAACACCCTGGTTCATT-3'; Hprt-Fwd, 5'-AGCCTAAGAT-GAGCGCAAGT-3', Rev, 5'-TTACTAGGCAGATGGCCACA-3'; Rorc-Fwd, 5'-TGCAAGACTCATCGACAAGG-3', Rev, 5'-AGGGATTCAACAT-CAGTGC-3'; Tbet-Fwd, 5'-TCAACCAGCACCAGACAGAG-3', Rev, 5'-AAACATCCTGTAATGGCTTGTG-3'; Il17a-Fwd, 5'-GCTCCA-GAAGGCCCTCAGA-3', Rev, 5'-CTTCCCTCCGCATTGACA-3'.

In vitro kinase assay. Purified recombinant mouse His-p38 α was activated or not by incubation with either 300 ng of active Zap70 (R&D Systems) or 1 μ g of active MKK6 at 30°C in 20 μ l of kinase buffer (20 mM Tris, pH 7.5, 20 mM MgCl₂, 1 mM dithiothreitol [DTT], 10 mM β -glycerophosphate, and 1 mM Na₃VO₄ and 50 μ M ATP). After 1 h, 1 μ g ATF2 or NFATc1 and 10 μ Ci [32 P]ATP were added and incubation proceeded for 45 min at 30°C. Phosphorylated products were resolved by SDS-PAGE, transferred to nitrocellulose membranes, and visualized with a Storm PhosphorImager (GE Healthcare).

Activation of the MAPK cascade p38 activation pathway. Purified CD4⁺ T cells were treated with sorbitol (0.6 M) for 30 min at 37°C in complete medium and washed once before plating. For activation with UV in vitro, cells were treated with 50 J/m² UVB and washed once with complete medium before plating. For mitogenic activation of the classical pathway, PMA was added in the cell culture at a concentration of 10 ng/ml in presence of ionomycin (1 μ g/ml).

UV treatment and analysis of mouse skin-resident T cells. The back and flanks of 6–8-wk-old B6 mice were shaved before exposure to the minimal erythema dose (MED) of UVA/UVB (\sim 9.6 kJ/m² from a bank of FS40 sunlamps, 60% UVB, 40% UVA, <1% UVC). 1 h later, the mice were euthanized and the skins harvested for analysis. To purify CD4⁺ T cells, irradiated or unirradiated full-thickness skin without subcutaneous tissue was incubated for 1.75 h at 37°C in RPMI containing 400 μ g/ml Liberase TL (Roche), at which time 0.1% DNase I (Sigma-Aldrich) was added (final concentration 0.05%) for an additional 15 min. Single-cell suspensions were prepared by sequential filtering through 100-, 70-, and 40- μ m nylon mesh, and then passage over Lympholyte M density gradients (Cedarlane) and centrifugation at 1,000 g for 20 min at room temperature. Finally, CD4⁺ T cells were purified by positive selection using MACS columns.

***C. rodentium* infection.** *C. rodentium* was prepared by selecting a single colony and culturing in LB broth overnight. 6–12-wk-old pathogen-free female C57BL/6 mice were inoculated via oral gavage with 200 μ l of the overnight culture. Colon biopsies were taken, formalin fixed, paraffin-embedded and H&E stained for histopathological analysis. Histological scoring was performed by two double-blinded, experienced observers. The groups were encoded, and in all cases a consensus was obtained. In the case of divergent scoring, a third observer decided upon the final interpretation.

Immunohistochemistry. Paraffin-embedded tissue sections (4 μ m) were analyzed using the avidin-biotin complex method (EnVision; Dako). Prior to incubation with primary antibody (rabbit polyclonal anti-CD3 [SP7; Abcam], rabbit polyclonal anti-T180/Y182 phospho-p38 [Cell Signaling Technology], or rabbit anti-pY323 p38 [ECM Biosciences]), antigen retrieval by heat pretreatment using citrate buffer (pH 6.1) was performed.

Triple immunofluorescence staining. Biopsies of psoriatic lesions were obtained from the tissue bank for inflammatory diseases, Heidelberg, Germany and from the Division of Dermatology, University Hospital Zurich, Switzerland. Written informed consent of each patient was collected. Tissue biopsies before ($n = 6$) or after ($n = 3$) a 9–24 d cycle of tri-weekly UVB irradiation with 311-nm narrow band light were fixed in formalin and embedded in paraffin. At the time of biopsy all patients received topical treatment (steroid containing topical creams). The following primary antibodies were used: rabbit anti-human CD3 (SP7; Abcam), mouse anti-human IRF4 (MUM1p; Dako), goat anti-human IL17A (R&D Systems), and rabbit anti-human p38 pY323 (ECM Biosciences). Isotype- and concentration-matched mouse and rabbit control mAb and normal rabbit Ig (Dako) and goat Ig (Dianova) served as negative controls. Staining was performed on 2- μ m paraffin sections of formalin-fixed sections. Antigen retrieval was achieved by steam cooking the slides in 1 mM EDTA (pH 9.0; Dako) for 30 min 10% Earle's balanced salt solution (Sigma-Aldrich) supplemented with 1% Hepes (Sigma-Aldrich) and 0.1% Saponin (Sigma-Aldrich), pH 7.4, was used as washing buffer. Primary antibody dilutions were prepared in antibody diluent (DCS) and incubated for 1 h at room temperature in a moist chamber. Biotinylated donkey anti-goat IgG Ab 1/200 (Jackson ImmunoResearch Laboratories), and sheep anti-mouse IgG Ab 1/250 (Binding Site), were used as secondary reagents for 30 min at room temperature, followed by Cy-3-conjugated streptavidin 1/1,000 (red fluorescence), DyLight488-conjugated donkey anti-sheep Ab 1/200 (green fluorescence), and Cy5-conjugated donkey anti-rabbit Ab 1/200 (all from Jackson ImmunoResearch Laboratories), for 30 min. Slides were viewed with a Laserscan microscope using suitable filter combinations provided by the manufacturer (Leica).

Statistical analysis. P values were calculated by Student's *t* test.

The authors thank Glenn Merlino and Cari Graff-Cherry for their assistance in treating mice with UV, Nicolas Bouladoux for his assistance in the *C. rodentium* experiments, and Remy Bosselut and Mark Udey for their critical comments and suggestions. The authors thank Jutta Scheuerer for expert technical assistance and Frank Bergmann for assistance in immunostaining.

This work was supported by the Intramural Research Program of the Center for Cancer Research, National Cancer Institute, National Institutes of Health. M.M. Gaida was supported by a fellowship from the German Research Foundation Ga-1818/1-1. The work of F. Lasitschka was in part funded by the German Research Foundation, SFB 938/TP Z2.

The authors declare no competing financial interests.

Submitted: 10 September 2013

Accepted: 10 April 2014

REFERENCES

- Aragão, A.Z., M.L. Nogueira, D.C. Granato, F.M. Simabuco, R.V. Honorato, Z. Hoffman, S. Yokoi, F.R. Laurindo, F.M. Squina, A.C. Zeri, et al. 2012. Identification of novel interaction between ADAM17 (a disintegrin and metalloprotease 17) and thioredoxin-1. *J. Biol. Chem.* 287:43071–43082. <http://dx.doi.org/10.1074/jbc.M112.364513>
- Aujla, S.J., Y.R. Chan, M. Zheng, M. Fei, D.J. Askew, D.A. Pociask, T.A. Reinhart, F. McAllister, J. Edeal, K. Gaus, et al. 2008. IL-22 mediates mucosal host defense against Gram-negative bacterial pneumonia. *Nat. Med.* 14:275–281. <http://dx.doi.org/10.1038/nm1710>
- Bettelli, E., Y. Carrier, W. Gao, T. Korn, T.B. Strom, M. Oukka, H.L. Weiner, and V.K. Kuchroo. 2006. Reciprocal developmental pathways for the generation of pathogenic effector TH17 and regulatory T cells. *Nature*. 441:235–238. <http://dx.doi.org/10.1038/nature04753>
- Blomberg, K.E., N. Boucheron, J.M. Lindvall, L. Yu, J. Raberger, A. Berglöf, W. Ellmeier, and C.E. Smith. 2009. Transcriptional signatures of Itk-deficient CD3+, CD4+ and CD8+ T-cells. *BMC Genomics*. 10:233. <http://dx.doi.org/10.1186/1471-2164-10-233>
- Brüstle, A., S. Heink, M. Huber, C. Rosenplänter, C. Stadelmann, P. Yu, E. Arpaia, T.W. Mak, T. Kamradt, and M. Lohoff. 2007. The development of inflammatory T(H)-17 cells requires interferon-regulatory factor 4. *Nat. Immunol.* 8:958–966. <http://dx.doi.org/10.1038/ni1500>
- Bry, L., and M.B. Brenner. 2004. Critical role of T cell-dependent serum antibody, but not the gut-associated lymphoid tissue, for surviving acute mucosal infection with *Citrobacter rodentium*, an attaching and effacing pathogen. *J. Immunol.* 172:433–441. <http://dx.doi.org/10.4049/jimmunol.172.1.433>
- Cho, M.L., J.H. Ju, K.W. Kim, Y.M. Moon, S.Y. Lee, S.Y. Min, Y.G. Cho, H.S. Kim, K.S. Park, C.H. Yoon, et al. 2007. Cyclosporine A inhibits IL-15-induced IL-17 production in CD4+ T cells via down-regulation of PI3K/Akt and NF-kappaB. *Immunol. Lett.* 108:88–96. <http://dx.doi.org/10.1016/j.imlet.2006.11.001>
- Chow, C.W., and R.J. Davis. 2000. Integration of calcium and cyclic AMP signaling pathways by 14-3-3. *Mol. Cell. Biol.* 20:702–712. <http://dx.doi.org/10.1128/MCB.20.2.702-712.2000>
- Chow, C.W., C. Dong, R.A. Flavell, and R.J. Davis. 2000. c-Jun NH(2)-terminal kinase inhibits targeting of the protein phosphatase calcineurin to NFATc1. *Mol. Cell. Biol.* 20:5227–5234. <http://dx.doi.org/10.1128/MCB.20.14.5227-5234.2000>
- Cristillo, A.D., and B.E. Bierer. 2002. Identification of novel targets of immunosuppressive agents by cDNA-based microarray analysis. *J. Biol. Chem.* 277:4465–4476. <http://dx.doi.org/10.1074/jbc.M108598200>
- Curtis, M.M., and S.S. Way. 2009. Interleukin-17 in host defence against bacterial, mycobacterial and fungal pathogens. *Immunology*. 126:177–185. <http://dx.doi.org/10.1111/j.1365-2567.2008.03017.x>
- Erkin, G., Y. Uğur, C.K. Güler, E. Aşan, P. Korkusuz, S. Sahin, and F. Kölemen. 2007. Effect of PUVA, narrow-band UVB and cyclosporin on inflammatory cells of the psoriatic plaque. *J. Cutan. Pathol.* 34:213–219. <http://dx.doi.org/10.1111/j.1600-0560.2006.00591.x>
- Farrow, M.A., E.Y. Kim, S.M. Wolinsky, and A.M. Sheehy. 2011. NFAT and IRF proteins regulate transcription of the anti-HIV gene, APOBEC3G. *J. Biol. Chem.* 286:2567–2577. <http://dx.doi.org/10.1074/jbc.M110.154377>
- Fitch, E., E. Harper, I. Skorcheva, S.E. Kurtz, and A. Blauvelt. 2007. Pathophysiology of psoriasis: recent advances on IL-23 and Th17 cytokines. *Curr. Rheumatol. Rep.* 9:461–467. <http://dx.doi.org/10.1007/s11926-007-0075-1>
- Galeazzi, F., P.A. Blennerhasset, B. Qiu, P.M. O'Byrne, and S.M. Collins. 1999. Cigarette smoke aggravates experimental colitis in rats. *Gastroenterology*. 117:877–883. [http://dx.doi.org/10.1016/S0016-5685\(99\)70346-X](http://dx.doi.org/10.1016/S0016-5685(99)70346-X)
- Ghosh, S., S.B. Koralov, I. Stevanovic, M.S. Sundrud, Y. Sasaki, K. Rajewsky, A. Rao, and M.R. Müller. 2010. Hyperactivation of nuclear factor of activated T cells 1 (NFAT1) in T cells attenuates severity of murine autoimmune encephalomyelitis. *Proc. Natl. Acad. Sci. USA*. 107:15169–15174. <http://dx.doi.org/10.1073/pnas.1009193107>
- Gómez del Arco, P., S. Martínez-Martínez, J.L. Maldonado, I. Ortega-Pérez, and J.M. Redondo. 2000. A role for the p38 MAP kinase pathway in the nuclear shuttling of NFATp. *J. Biol. Chem.* 275:13872–13878. <http://dx.doi.org/10.1074/jbc.275.18.13872>
- Graneli-Piperno, A., K. Inaba, and R.M. Steinman. 1984. Stimulation of lymphokine release from T lymphoblasts. Requirement for mRNA synthesis and inhibition by cyclosporin A. *J. Exp. Med.* 160:1792–1802. <http://dx.doi.org/10.1084/jem.160.6.1792>
- Grundmann-Kollmann, M., H. Martin, R. Ludwig, S. Klein, W.H. Boehncke, D. Hoelzer, R. Kaufmann, and M. Podda. 2002. Narrowband UV-B phototherapy in the treatment of cutaneous graft versus host disease. *Transplantation*. 74:1631–1634. <http://dx.doi.org/10.1097/00007890-200212150-00023>
- Jirmanova, L., D.N. Sarma, D. Jankovic, P.R. Mittelstadt, and J.D. Ashwell. 2009. Genetic disruption of p38alpha Tyr323 phosphorylation prevents T-cell receptor-mediated p38alpha activation and impairs interferon-gamma production. *Blood*. 113:2229–2237. <http://dx.doi.org/10.1182/blood-2008-04-153304>
- Jirmanova, L., M.L. Giardino Torchia, N.D. Sarma, P.R. Mittelstadt, and J.D. Ashwell. 2011. Lack of the T cell-specific alternative p38 activation pathway reduces autoimmunity and inflammation. *Blood*. 118:3280–3289. <http://dx.doi.org/10.1182/blood-2011-01-333039>
- Johnson, E., and S.W. Barthold. 1979. The ultrastructure of transmissible murine colonic hyperplasia. *Am. J. Pathol.* 97:291–313.
- Kaminuma, O., F. Kitamura, N. Kitamura, T. Hiroi, H. Miyoshi, A. Miyawaki, and S. Miyatake. 2008. Differential contribution of NFATc2 and NFATc1 to TNF-alpha gene expression in T cells. *J. Immunol.* 180:319–326. <http://dx.doi.org/10.4049/jimmunol.180.1.319>
- Kebir, H., K. Kreyborg, I. Ifergan, A. Dodelet-Devillers, R. Cayrol, M. Bernard, F. Giuliani, N. Arbour, B. Becher, and A. Prat. 2007. Human

- TH17 lymphocytes promote blood-brain barrier disruption and central nervous system inflammation. *Nat. Med.* 13:1173–1175. <http://dx.doi.org/10.1038/nm1651>
- Koike, T., H. Yamagishi, Y. Hatanaka, A. Fukushima, J.W. Chang, Y. Xia, M. Fields, P. Chandler, and M. Iwashima. 2003. A novel ERK-dependent signaling process that regulates interleukin-2 expression in a late phase of T cell activation. *J. Biol. Chem.* 278:15685–15692. <http://dx.doi.org/10.1074/jbc.M210829200>
- Komiyama, Y., S. Nakae, T. Matsuki, A. Nambu, H. Ishigame, S. Kakuta, K. Sudo, and Y. Iwakura. 2006. IL-17 plays an important role in the development of experimental autoimmune encephalomyelitis. *J. Immunol.* 177:566–573. <http://dx.doi.org/10.4049/jimmunol.177.1.566>
- Korn, T., E. Bettelli, M. Oukka, and V.K. Kuchroo. 2009. IL-17 and Th17 Cells. *Annu. Rev. Immunol.* 27:485–517. <http://dx.doi.org/10.1146/annurev.immunol.021908.132710>
- Leonardi, C., R. Matheson, C. Zachariae, G. Cameron, L. Li, E. Edson-Heredia, D. Braun, and S. Banerjee. 2012. Anti-interleukin-17 monoclonal antibody ixekizumab in chronic plaque psoriasis. *N. Engl. J. Med.* 366:1190–1199. <http://dx.doi.org/10.1056/NEJMoa1109997>
- Lohoff, M., H.W. Mittrücker, S. Precht, S. Bischof, F. Sommer, S. Kock, D.A. Ferrick, G.S. Duncan, A. Gessner, and T.W. Mak. 2002. Dysregulated T helper cell differentiation in the absence of interferon regulatory factor 4. *Proc. Natl. Acad. Sci. USA.* 99:11808–11812. <http://dx.doi.org/10.1073/pnas.182425099>
- Loser, K., A. Mehling, S. Loeser, J. Apelt, A. Kuhn, S. Grabbe, T. Schwarz, J.M. Penninger, and S. Beissert. 2006. Epidermal RANKL controls regulatory T-cell numbers via activation of dendritic cells. *Nat. Med.* 12:1372–1379. <http://dx.doi.org/10.1038/nm1518>
- Lu, L., J. Wang, F. Zhang, Y. Chai, D. Brand, X. Wang, D.A. Horwitz, W. Shi, and S.G. Zheng. 2010. Role of SMAD and non-SMAD signals in the development of Th17 and regulatory T cells. *J. Immunol.* 184:4295–4306. <http://dx.doi.org/10.4049/jimmunol.0903418>
- Macian, F. 2005. NFAT proteins: key regulators of T-cell development and function. *Nat. Rev. Immunol.* 5:472–484. <http://dx.doi.org/10.1038/nri1632>
- Matsumoto, M., T. Sudo, T. Saito, H. Osada, and M. Tsujimoto. 2000. Involvement of p38 mitogen-activated protein kinase signaling pathway in osteoclastogenesis mediated by receptor activator of NF-kappa B ligand (RANKL). *J. Biol. Chem.* 275:31155–31161. <http://dx.doi.org/10.1074/jbc.M001229200>
- Mittelstadt, P.R., H. Yamaguchi, E. Appella, and J.D. Ashwell. 2009. T cell receptor-mediated activation of p38alpha by mono-phosphorylation of the activation loop results in altered substrate specificity. *J. Biol. Chem.* 284:15469–15474. <http://dx.doi.org/10.1074/jbc.M901004200>
- Mudter, J., J. Yu, C. Zufferey, A. Brüstle, S. Wirtz, B. Weigmann, A. Hoffman, M. Schenk, P.R. Galle, H.A. Lehr, et al. 2011. IRF4 regulates IL-17A promoter activity and controls ROR-gamma-t-dependent Th17 colitis in vivo. *Inflam. Bowel Dis.* 17:1343–1358. <http://dx.doi.org/10.1002/ibd.21476>
- Nakae, S., A. Nambu, K. Sudo, and Y. Iwakura. 2003. Suppression of immune induction of collagen-induced arthritis in IL-17-deficient mice. *J. Immunol.* 171:6173–6177. <http://dx.doi.org/10.4049/jimmunol.171.11.6173>
- Noubade, R., D.N. Kremontsov, R. Del Rio, T. Thornton, V. Nagaleekar, N. Saligrama, A. Spitzack, K. Spach, G. Sabio, R.J. Davis, et al. 2011. Activation of p38 MAPK in CD4 T cells controls IL-17 production and autoimmune encephalomyelitis. *Blood.* 118:3290–3300. <http://dx.doi.org/10.1182/blood-2011-02-336552>
- Papp, K.A., C. Leonardi, A. Menter, J.P. Ortonne, J.G. Krueger, G. Kricorian, G. Aras, J. Li, C.B. Russell, E.H. Thompson, and S. Baumgartner. 2012. Brodalumab, an anti-interleukin-17-receptor antibody for psoriasis. *N. Engl. J. Med.* 366:1181–1189. <http://dx.doi.org/10.1056/NEJMoa1109017>
- Pearson, G., F. Robinson, T. Beers Gibson, B.E. Xu, M. Karandikar, K. Berman, and M.H. Cobb. 2001. Mitogen-activated protein (MAP) kinase pathways: regulation and physiological functions. *Endocr. Rev.* 22:153–183.
- Peng, S.L., A.J. Gerth, A.M. Ranger, and L.H. Glimcher. 2001. NFATc1 and NFATc2 together control both T and B cell activation and differentiation. *Immunity.* 14:13–20. [http://dx.doi.org/10.1016/S1074-7613\(01\)00085-1](http://dx.doi.org/10.1016/S1074-7613(01)00085-1)
- Pernis, A.B. 2009. Th17 cells in rheumatoid arthritis and systemic lupus erythematosus. *J. Intern. Med.* 265:644–652. <http://dx.doi.org/10.1111/j.1365-2796.2009.02099.x>
- Poggi, A., S. Catellani, A. Musso, and M.R. Zocchi. 2009. Gammadelta T lymphocytes producing IFN-gamma and IL-17 in response to Candida albicans or mycobacterial antigens: possible implications for acute and chronic inflammation. *Curr. Med. Chem.* 16:4743–4749. <http://dx.doi.org/10.2174/092986709789878238>
- Porter, C.M., M.A. Havens, and N.A. Clipstone. 2000. Identification of amino acid residues and protein kinases involved in the regulation of NFATc subcellular localization. *J. Biol. Chem.* 275:3543–3551. <http://dx.doi.org/10.1074/jbc.275.5.3543>
- Rácz, E., E.P. Prens, D. Kurek, M. Kant, D. de Ridder, S. Mourits, E.M. Baerveldt, Z. Ozgur, W.F. van Ijcken, J.D. Laman, et al. 2011. Effective treatment of psoriasis with narrow-band UVB phototherapy is linked to suppression of the IFN and Th17 pathways. *J. Invest. Dermatol.* 131:1547–1558. <http://dx.doi.org/10.1038/jid.2011.53>
- Round, J.L., L.A. Humphries, T. Tomassian, P. Mittelstadt, M. Zhang, and M.C. Miceli. 2007. Scaffold protein Dlg1 coordinates alternative p38 kinase activation, directing T cell receptor signals toward NFAT but not NF-kappaB transcription factors. *Nat. Immunol.* 8:154–161. <http://dx.doi.org/10.1038/ni1422>
- Salvador, J.M., M.C. Hollander, A.T. Nguyen, J.B. Kopp, L. Barisoni, J.K. Moore, J.D. Ashwell, and A.J.J. Fornace Jr. 2002. Mice lacking the p53-effector gene Gadd45a develop a lupus-like syndrome. *Immunity.* 16:499–508. [http://dx.doi.org/10.1016/S1074-7613\(02\)00302-3](http://dx.doi.org/10.1016/S1074-7613(02)00302-3)
- Salvador, J.M., P.R. Mittelstadt, T. Guszczynski, T.D. Copeland, H. Yamaguchi, E. Appella, A.J.J. Fornace Jr., and J.D. Ashwell. 2005. Alternative p38 activation pathway mediated by T cell receptor-proximal tyrosine kinases. *Nat. Immunol.* 6:390–395. <http://dx.doi.org/10.1038/ni1177>
- Sato, K., F. Miyoshi, K. Yokota, Y. Araki, Y. Asanuma, Y. Akiyama, K. Yoh, S. Takahashi, H. Aburatani, and T. Mimura. 2011. Marked induction of c-Maf protein during Th17 cell differentiation and its implication in memory Th cell development. *J. Biol. Chem.* 286:14963–14971. <http://dx.doi.org/10.1074/jbc.M111.218867>
- Schwarz, D.A., C.D. Katayama, and S.M. Hedrick. 1998. Schlafen, a new family of growth regulatory genes that affect thymocyte development. *Immunity.* 9:657–668. [http://dx.doi.org/10.1016/S1074-7613\(00\)80663-9](http://dx.doi.org/10.1016/S1074-7613(00)80663-9)
- Silva-Santos, B. 2011. gamma delta cells making IL-17. *Blood.* 118:3–5. <http://dx.doi.org/10.1182/blood-2011-05-351726>
- Symonds, E.L., C.U. Riedel, D. O'Mahony, S. Laphorne, L. O'Mahony, and F. Shanahan. 2009. Involvement of T helper type 17 and regulatory T cell activity in Citrobacter rodentium invasion and inflammatory damage. *Clin. Exp. Immunol.* 157:148–154. <http://dx.doi.org/10.1111/j.1365-2249.2009.03934.x>
- Tominaga, N., K. Ohkusu-Tsukada, H. Udono, R. Abe, T. Matsuyama, and K. Yui. 2003. Development of Th1 and not Th2 immune responses in mice lacking IFN-regulatory factor-4. *Int. Immunol.* 15:1–10. <http://dx.doi.org/10.1093/intimm/dxg001>
- Tsuda, K., K. Yamanaka, H. Kitagawa, T. Akeda, M. Naka, K. Niwa, T. Nakanishi, M. Kakeda, E.C. Gabazza, and H. Mizutani. 2012. Calcineurin inhibitors suppress cytokine production from memory T cells and differentiation of naïve T cells into cytokine-producing mature T cells. *PLoS ONE.* 7:e31465. <http://dx.doi.org/10.1371/journal.pone.0031465>
- Veldhoen, M., K. Hirota, A.M. Westendorf, J. Buer, L. Dumoutier, J.C. Renaud, and B. Stockinger. 2008. The aryl hydrocarbon receptor links TH17-cell-mediated autoimmunity to environmental toxins. *Nature.* 453:106–109. <http://dx.doi.org/10.1038/nature06881>
- Walters, I.B., M. Ozawa, I. Cardinale, P. Gilleaudeau, W.L. Trepicchio, J. Bliss, and J.G. Krueger. 2003. Narrowband (312-nm) UV-B suppresses interferon gamma and interleukin (IL) 12 and increases IL-4 transcripts: differential regulation of cytokines at the single-cell level. *Arch. Dermatol.* 139:155–161. <http://dx.doi.org/10.1001/archderm.139.2.155>
- Weatherhead, S.C., P.M. Farr, D. Jamieson, J.S. Hallinan, J.J. Lloyd, A. Wipat, and N.J. Reynolds. 2011. Keratinocyte apoptosis in epidermal remodeling and clearance of psoriasis induced by UV radiation. *J. Invest. Dermatol.* 131:1916–1926. <http://dx.doi.org/10.1038/jid.2011.134>
- Wu, C.C., S.C. Hsu, H.M. Shih, and M.Z. Lai. 2003. Nuclear factor of activated T cells c is a target of p38 mitogen-activated protein kinase in T cells. *Mol. Cell. Biol.* 23:6442–6454. <http://dx.doi.org/10.1128/MCB.23.18.6442-6454.2003>

- Yang, X.O., B.P. Pappu, R. Nurieva, A. Akimzhanov, H.S. Kang, Y. Chung, L. Ma, B. Shah, A.D. Panopoulos, K.S. Schluns, et al. 2008. T helper 17 lineage differentiation is programmed by orphan nuclear receptors ROR alpha and ROR gamma. *Immunity*. 28:29–39. <http://dx.doi.org/10.1016/j.immuni.2007.11.016>
- Yoshida, H., H. Nishina, H. Takimoto, L.E. Marengère, A.C. Wakeham, D. Bouchard, Y.Y. Kong, T. Ohteki, A. Shahinian, M. Bachmann, et al. 1998. The transcription factor NF-ATc1 regulates lymphocyte proliferation and Th2 cytokine production. *Immunity*. 8:115–124. [http://dx.doi.org/10.1016/S1074-7613\(00\)80464-1](http://dx.doi.org/10.1016/S1074-7613(00)80464-1)
- Zhang, C., J. Zhang, B. Yang, and C. Wu. 2008. Cyclosporin A inhibits the production of IL-17 by memory Th17 cells from healthy individuals and patients with rheumatoid arthritis. *Cytokine*. 42:345–352. <http://dx.doi.org/10.1016/j.cyto.2008.03.006>
- Zhou, L., I.I. Ivanov, R. Spolski, R. Min, K. Shenderov, T. Egawa, D.E. Levy, W.J. Leonard, and D.R. Littman. 2007. IL-6 programs T(H)-17 cell differentiation by promoting sequential engagement of the IL-21 and IL-23 pathways. *Nat. Immunol.* 8:967–974. <http://dx.doi.org/10.1038/ni1488>